



Science Arts & Métiers (SAM)

is an open access repository that collects the work of Arts et Métiers Institute of Technology researchers and makes it freely available over the web where possible.

This is an author-deposited version published in: <https://sam.ensam.eu>
Handle ID: <http://hdl.handle.net/10985/26207>



This document is available under CC BY license

To cite this version :

Arthur PATÉ, Maxime PETEL, Nesrine BELHASSEN, Delphine CHADEFAUX - Radiated Sound and Transmitted Vibration Following the Ball/Racket Impact of a Tennis Serve - Vibration - Vol. 7, n°4, p.894-911 - 2024

Any correspondence concerning this service should be sent to the repository

Administrator : scienceouverte@ensam.eu



Article

Radiated Sound and Transmitted Vibration Following the Ball/Racket Impact of a Tennis Serve

Arthur Paté ^{1,*},[†] , Maxime Petel ², Nesrine Belhassen ² and Delphine Chadeaux ^{2,*},[†] 

¹ Univ. Lille, CNRS, Centrale Lille, Junia, Univ. Polytechnique Hauts-de-France, UMR 8520—IEMN, F-59000 Lille, France

² Université Sorbonne Paris Nord, Arts et Métiers Institute of Technology, IBHGC-Institut de Biomécanique Humaine Georges Charpak, HESAM Université, F-75013 Paris, France

* Correspondence: arthur.pate@isen.fr (A.P.); delphine.chadeaux@univ-paris13.fr (D.C.)

[†] These authors contributed equally to this work.

Abstract: Shock-induced vibrations transmitted from the racket to the tennis player's upper limb have interested researchers, whether for investigating their effect on injury risk, or for designing new equipment. Measuring these vibrations is, however, very challenging in an ecological playing situation: sensors must be of very high quality in order to precisely measure high-energy and broad-frequency signals, as well as non-invasive in order to allow the players to perform their usual movements. The working hypothesis of this paper is that contactless sound recordings of the ball/racket impact carry the same information as direct vibratory measurements. The present study focuses on the tennis serve, as being tennis' most energy-demanding stroke, therefore possibly being the most traumatic stroke for the upper limb. This article aims (a) to evaluate the propagation of vibration from the racket to the upper limb; and (b) to identify correlations with acoustic signals collected simultaneously. Eight expert tennis players performed serves with three rackets and two ball spin effects. Accelerometers measured the vibration on the racket and at five locations on the upper limb, and a microphone measured the impact sound. Resulting signals were analyzed in terms of energy and spectral descriptors. Results showed that flat serves produced louder sounds, higher vibration levels, lower acoustic spectral centroids, and higher vibratory spectral centroids than kick serves. The racket only had a marginal influence. Similarities between acoustic and vibratory measurements were found (levels were correlated), but so were differences (spectral centroids tended to be negatively correlated), encouraging further studies on the link between sound and vibration for the in situ measurement of shock-induced vibration.

Keywords: tennis; sound; acoustic; vibration; in-situ measurements; sport



Citation: Paté, A.; Petel, M., Belhassen, N.; Chadeaux, D. Radiated Sound and Transmitted Vibration Following the Ball/Racket Impact of a Tennis Serve. *Vibration* **2024**, *7*, 894–911. <https://doi.org/10.3390/vibration7040047>

Academic Editors: Aleksandar Pavic and Xavier Chiementin

Received: 19 August 2024

Revised: 25 September 2024

Accepted: 27 September 2024

Published: 30 September 2024



Copyright: © 2024 by the authors. Licensee MDPI, Basel, Switzerland. This article is an open access article distributed under the terms and conditions of the Creative Commons Attribution (CC BY) license (<https://creativecommons.org/licenses/by/4.0/>).

1. Introduction

Tennis practice, implying shock-induced vibrations propagating from the racket to the player's upper limb, has intuitively been related to injury risk [1,2]. As a result, manufacturers have upgraded sport equipment (e.g., string material and tension, frame rigidity, antivibration systems) with respect to players' demands and feedback, working towards the minimization of the amount of vibration reaching the human body, while maintaining maneuverability and therefore performance [3]. Nevertheless, there is no clear scientific evidence that links the amount of transmitted vibration to the risk of injury. Indeed, although recent works have developed wearable devices to extract biomechanical information and derive hypotheses regarding a risk of injury [4], no direct in vivo evaluation of the mechanical load applied to the anatomical elements during sport practice can be performed, so the risks of damage can not be derived by simple comparison of such measurements with available data relating to, e.g., the mechanical resistance of human tissue.

To overcome this limitation, a possible perspective involves the development of biomechanical models of the hand-held racket, fed by measurements collected during

sport practice [5,6]. Data collection during sport practice requires sensors that induce no modification to the player's gestures and feeling. Kinematic data are reachable through inertial sensors [7] or motion capture systems [8]. However, dynamics are more difficult to estimate because of the high shock intensity. Numerous studies have outlined the effect of the player's level [1,9], grip force [6,10] and position [4], the impact location [1], the ball spin [4], and obviously the racket properties [4,10,11] on the racket and upper limb acceleration. Although the reported accelerations are influenced by the playing conditions, the magnitudes have remained generally consistent across the literature. The peak accelerations at the racket frame, wrist, and elbow can be estimated at approximately 100 g, 25 g, and 10 g, respectively. Furthermore, by definition, the shock duration is very short, and has been reported to be a few tens of ms. Finally, modal analyses of sporting equipment have revealed spectral content up to about 1500 Hz [6]. Such values underline the need for high-performance sensors on the racket. Miniature sensors have to be used to add a negligible mass to the racket, and their range of measurement has to be at least 100 g. The acquisition board should allow a sampling frequency higher than 3000 Hz. Finally, the whole system has to be integrated in an on-board apparatus to give the player freedom of movement. To date, no wireless sensor of this type exists, suggesting the use of wired accelerometers commonly used for industrial purposes to equip the racket. On the contrary, existing wireless sensors are valid to measure the vibration propagation through the upper limb. Consequently, although measurement techniques are making steady progress, it is not possible today to design an experimental setup that aims to evaluate the equipment's quality without attaching additional devices onto the player's body. Even if the devices in question are sufficiently light and non-intrusive to allow for the practice of sport, the experiment is not an actual ecological situation. To reach an ecological situation, measurements should be carried out with no contact and no disturbance of the sport practice. As the sound radiated by the racket-ball impact is a projection of the equipment's vibratory behavior, our hypothesis is that recording the sound radiated by the impact may replace the direct measurement of vibration of the racket.

The aim of this article is twofold: (a) to evaluate the shock-induced vibration propagation from the racket up to the player's shoulder; and (b) to identify correlations with acoustic signals collected simultaneously. For this purpose, the present study focuses on the practice of tennis serve under various conditions (i.e., with different rackets and using different ball spin conditions) in order to cover a certain diversity of situations encountered in tennis playing. This particular stroke was specifically chosen because of its supposed traumatic effect on the upper limb, since it is the most energy-demanding stroke [12]. Moreover, to the authors' knowledge, no study has yet reported vibration propagation from the racket to the player's shoulder following a tennis serve. Finally, this stroke has a certain repeatability in comparison to, e.g., backhand and forehand strokes: the player's placement and the kinematics and timing of the serve gesture are less prone to variations.

Section 2 presents the experimental setup and method, and Section 3 presents the analysis method. The results are presented in Section 4 and discussed in Section 5, before drawing conclusions in Section 6.

2. Materials and Methods

2.1. Participants

Eight right-handed male tennis players (26 ± 5 years old) took part in the experiment. Throughout the remainder of the article, they are numbered from S1 through S8. They all practice or practiced tennis at a high level, and still had at least a French 3/6 ranking (equivalent to an Universal Tennis Rating of 9–9.5, and an International Tennis Number of 3) at the time of the experiment. None reported being injured at the time of the experiments or in the previous six months. Due to the limited availability of the tennis court, no more players were involved in the study, and it was assumed that their proven experience was representative of the population of expert players. This study received approval from a national ethics committee (number IRB00012476-2022-24-05-184).

2.2. Rackets

Three rackets were chosen according to the expertise of a former professional tennis player. The rackets differed in their perceived vibratory behavior: *R1* was perceived as the least vibratory of his rackets, and *R3* as the most vibratory, with *R2* lying in between. Rackets were deliberately chosen for their assumed different vibratory behaviors, which were expected to lead to measurable differences; rackets were chosen based on this expert player's perception, because in the long run we aim to match the vibratory and acoustical measurements with the perceptions of other players. Prior to the experiment, all rackets were strung with Head Hawk strings (gauge 1.3 mm), and set to the same tension (23.5 kg in both directions). Due to the limited availability of rackets, it was not possible to perform mechanical measurements prior to the tests (e.g., modal analysis, inertia, balance, weight, etc.).

2.3. Experimental Procedure

Each player was first asked to perform a short, freestyle warm-up (typically 5 to 10 min), before being equipped with sensors (see Section 2.4). The first racket was then equipped and handed over to the player. The player was asked to perform a series of five *flat* and five *kick* serves (corresponding, respectively, to typical effects for first and second serves during regular tennis matches). Players were asked to serve from the advantage side (see Figure 1). No validation criterion was set, so that each serve was recorded, except for serves far outside the target. No time limit was set and the players were free to serve at their own pace. After the series of serves was completed with one racket, a 5 min break was employed prior to equipping the next racket. Then, the very same procedure was applied with the other two rackets successively. The order of both rackets and ball spin conditions was balanced across players in order to avoid fatigue or learning effects.

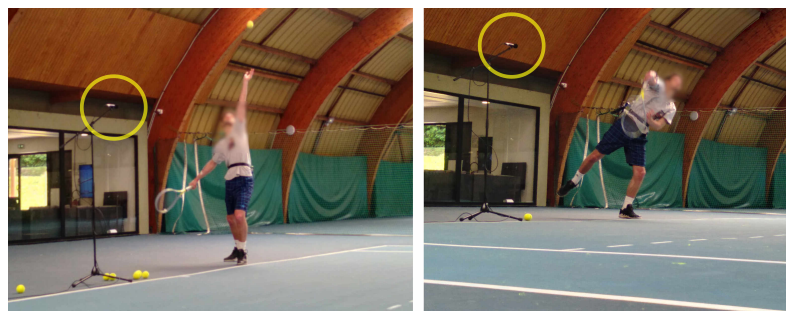


Figure 1. A serve performed by a player (**left**, before hitting the ball; **right**, after hitting the ball). The yellow circle indicates the position of the microphone for the acoustic measurements.

2.4. Vibration Measurements

Rackets were equipped with four wired accelerometers (single-axis, maximum acceleration ± 500 g peak, operating frequency range [1–8000] Hz, mass 0.6 g, dimensions: $3.6 \times 11.4 \times 6.4$ mm, ICP, sensitivity 10 mV/g, manufactured by PCB Piezotronics, Buffalo, NY, USA, sampling frequency $F_{s,vib} = 44,100$ Hz). These four accelerometers were placed on the frame, two just above the handle (abbreviated *H* in the following), and the other two halfway down the length of the head of the racket (i.e., on the side of the racket, abbreviated *S* in the following): see yellow circles in Figure 2a. For each pair of accelerometers on the racket (one pair near the handle, one pair on the side), one measured acceleration was obtained within the plane of the racket (abbr. *IP*), and the other was from out of this plane (abbr. *OP*). In the remainder of the article, the accelerometers on the racket are referred to as *HIP*, *HOP*, *SIP*, and *SOP*, measuring in-plane vibrations on the handle, out-of-plane vibrations on the handle, in-plane vibrations on the side of the frame, and out-of-plane vibrations on the side of the frame, respectively. These accelerometers were connected through wires running along the player's body down to a box fixed at his belt, containing acquisition cards connected to a nano-computer. This nano-computer was driven from a

remote laptop computer to control the acquisitions.

Five wireless accelerometers (three axes, sensitivity 13 bits, maximum acceleration ± 200 g, mass 9.5 g, dimensions $42 \times 27 \times 11$ mm, Blue Trident IMU manufactured by Vicon, Oxford, UK, sampling frequency $F_{s,vib} = 1600$ Hz) were placed and fixed with adhesive dermatological tape on the player's right upper limb. Their positions (visible in Figure 2b) were set to be as close as possible to the distal and proximal extremities of the forearm, distal and proximal extremities of the upper-arm, and on the acromion. In the remainder of the article, these accelerometers will be referred to as *FA_dist*, *FA_prox*, *UA_dist*, *UA_prox*, and *Acromion*, respectively. Their signals were sent over a bluetooth protocol managed by the dedicated Capture-U application, Vicon, Oxford, UK.

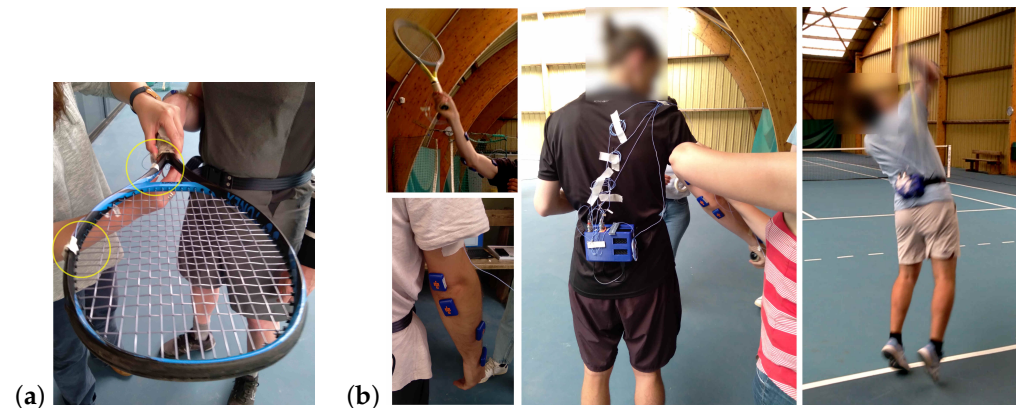


Figure 2. (a) Circled in yellow, the position of the 4 accelerometers on the racket: 2 on the side of the frame (named *SIP* and *SOP*), 2 on the top of the handle (named *HIP* and *HOP*). (b) Wireless accelerometers on the upper limb of the player, and wires running from the accelerometers on the racket to a box containing the acquisition card, carried by the player as a waistbag. Note that additional wireless accelerometers are visible on the player's upper limb. These were not used in this study.

2.5. Acoustic Measurements

Acoustic measurements were performed by placing a microphone (cardioid directivity, sensitivity 15 mV/Pa, advertised operating range [20–20,000] Hz, model KM184 manufactured by Neumann, Berlin, Germany) at the same height as, and 1 m away from, the player's right ear (see the yellow circles in Figure 1). The microphone was connected to a sound interface (Scarlett 2i2, manufactured by Focusrite, quantization 24 bits, sampling frequency $F_{s,acou} = 44,100$ Hz) for analog-to-digital conversion.

3. Analysis

3.1. Analysis of Vibratory Signals

Vibratory signals from all 240 measurements (eight players \times two ball spin \times three rackets \times five trials) and from all nine accelerometers were analyzed. First, the signals were trimmed to 300 ms segments in order to keep windows with satisfactory signal-to-noise ratios, from 100 ms before to 200 ms after the acceleration peak, assumed to happen at the time of impact. The discrete spectrum of each signal was computed through a fast Fourier transform for between-racket and between-effect comparison. In parallel, descriptors were computed from the segmented signals.

As a descriptor of energy, the *RMS* value was defined as

$$RMS = \sqrt{\frac{1}{N_{vib}} \sum_{n=1}^{N_{vib}} v^2(n)}, \quad (1)$$

where $v(n)$ is the discrete vibratory signal as a time series of N_{vib} points. As a descriptor of spectral content, the spectral centroid SC was defined as

$$SC = \frac{\sum_{k=1}^{N_{vib}} f_k a_k}{\sum_{k=1}^{N_{vib}} a_k}, \quad (2)$$

where f_k and a_k , respectively, are the k -th frequency and amplitude of the discrete spectrum of $v(n)$, computed over N_{vib} points. Prior to computing the spectral centroids for the vibratory measurements, the signals were first passed through a band-pass filter with zero phase shift (order-4, high-pass Butterworth filter) in order to keep only the [15–1000] Hz frequency range and get rid of kinematic data in the lower-frequency range and noise in the high frequencies.

3.2. Analysis of Acoustic Signals

The microphone was calibrated with a sound level meter (01dB Fusion fitted with a 01dB 40CE microphone), so that after correction, each audio recording had values expressed in Pascals (p). Acoustic signals from all 240 measurements were analyzed. Each recording was trimmed to the interval ranging from 100 ms before impact to 300 ms after impact (detected as the time at which the maximum acoustic amplitude was reached), in order to keep the impulsive part of the acoustic signal only and discard the effects of the environment (reverberation due to reflections over walls and ceiling, or resonances due to the dimensions of the indoor court). Each trimmed signal was then filtered by an order-5 Butterworth high-pass filter with cutoff frequency 50 Hz, in order to remove spectral contributions from the environment (mainly low-frequency resonances of the indoor court).

The discrete spectrum of each filtered signal was computed through a fast Fourier transform for between-racket and between-effect comparison. In parallel, two audio descriptors were extracted from the time series, targeting energetic (sound pressure level) and spectral (spectral centroid) content description, for comparison with the vibratory descriptors.

The sound pressure level L was classically defined from the acoustic pressure $p(n)$ as

$$L = 20 \log_{10} \left(\frac{\sqrt{\frac{1}{N_{acou}} \sum_{n=1}^{N_{acou}} p^2(n)}}{p_{ref}} \right), \quad (3)$$

where $p(n)$ is the discrete-time signal indexed with n the sample number, N_{acou} is the total number of samples in the signal, and p_{ref} is the classical reference pressure ($p_{ref} = 2 \times 10^{-5}$ Pa).

The spectral centroid SC was computed according to Equation (2), based on the whole audio frequency range, i.e., from 0 (keeping in mind that the band [0–50] Hz was filtered out) to 22,050 Hz (half the sampling frequency).

3.3. Statistics

As one of the objectives of this study is to evaluate the shock-induced vibration and radiated sound under various conditions, it is of interest to examine the influence of these conditions on the observed features. Statistics were therefore computed to assess the influence of two factors (*racket* and *ball spin*) on the vibratory and acoustic descriptors.

All distributions for vibratory descriptors (RMS and SC) were first tested for normality with a Shapiro–Wilk test, and for sphericity with a Mauchly test. All distributions were found to be normal, and the sphericity conditions for RM-ANOVAs were met. Therefore, RM-ANOVAs were performed with factors *racket* (three levels: R_1 , R_2 , R_3) and *ball spin* (two levels: *flat*, *kick*) for both RMS and SC descriptors, and for each accelerometer.

Similarly, all distributions for acoustic descriptors (RMS and SC) were tested and found to be normal, and the sphericity conditions for the RM-ANOVAs were met. RM-ANOVAs were thus run with the same two factors.

In addition, it was investigated as to whether the vibration signals differed according to sensor location. For this purpose, vibratory descriptors of each accelerometer were merged across player, racket, and ball spin. The resulting distribution did not prove to be normal according to the Shapiro–Wilk test. Therefore, one Kruskal–Wallis test was performed in order to compare the RMS (resp. SC) values of accelerometers *FA_dist*, *FA_prox*, *UA_dist*, *UA_prox*, and *Acromion*; and another was performed in order to compare the RMS (resp. SC) values of *HIP*, *HOP*, *SIP*, and *SOP*.

Whenever relevant, post-hoc tests followed the main tests just described, namely Tukey HSD tests following the RM-ANOVAs, and Mann–Whitney tests following the Kruskal–Wallis tests. For all statistical tests, the significance level was deemed to be reached when the *p*-value was lower than 0.05.

4. Results

4.1. Inter- and Intra-Player Variability

Figures 3 and 4, respectively, show the individual (at the trial and player levels) and average values for the sound level *L* and the vibratory RMS level measured at the *FA_prox* position. The following phenomena hold for SC and for the other accelerometer positions, not shown here.

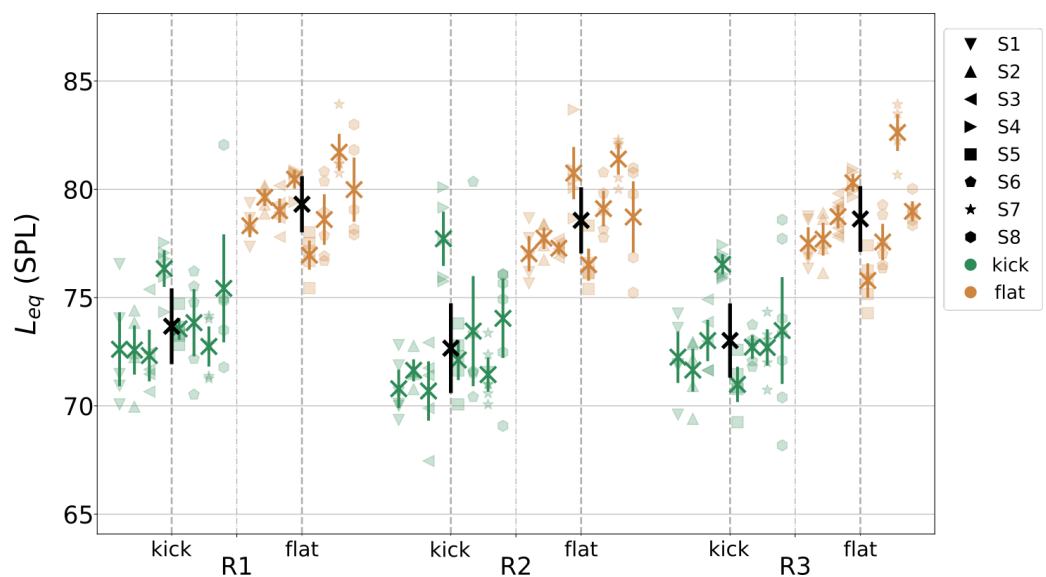


Figure 3. Sound pressure level (*L*) values computed on each trial, for each player, racket, and ball spin. For each racket (*R1*, *R2*, and *R3* from left to right), values are ordered according to ball spin: *kick* (green, left) and *flat* (copper, right). The values of each player are represented by a single marker. For each player, a cross indicates the mean, and a vertical bar spans the 95% confidence interval around the mean. The black cross and vertical lines indicate the mean and 95% confidence interval around the mean, computed across all players.

Some players stood out from the others, highlighting individual behaviors and characteristics: this was the case, e.g., for *S4* who constantly produced serves with a higher sound level, or for *S5*, who always showed the lowest vibratory RMS values, with a very high repetability (narrow 95% confidence interval).

As a further illustration of each player's signature, it can be observed that, for both acoustic and vibratory descriptors, the inter-player variability (up to 8 dB between mean values for the sound level, and up to 12 g for the RMS vibratory values) was larger than the intra-player variability (with 95% confidence intervals up to 5 dB for the sound level, and up to 10 g for the RMS vibratory values).

Besides inter-player variability, *ball spin* and to a lesser extent *racket* seemed to be associated with different descriptor values. The next two sections investigate this in detail.

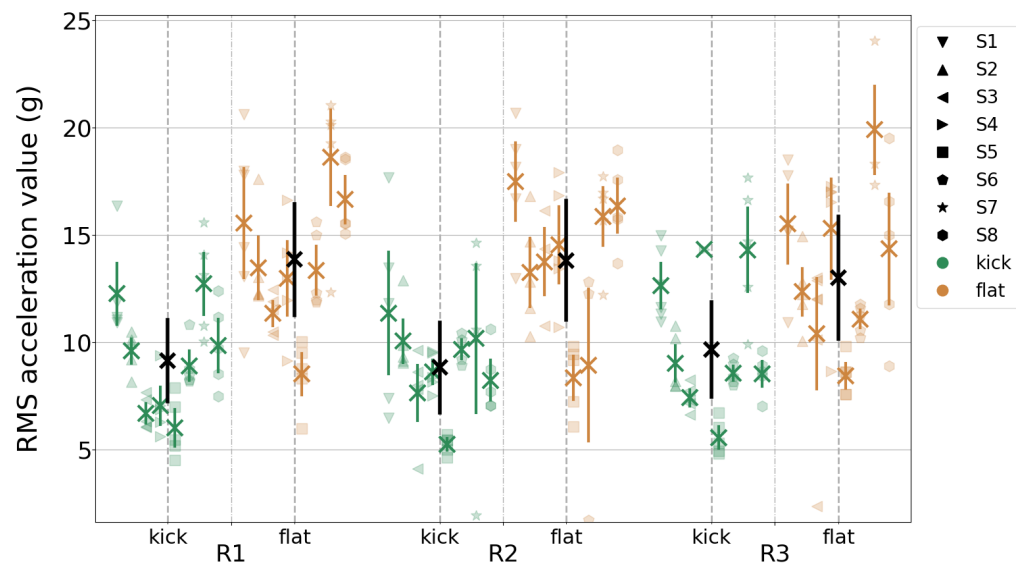


Figure 4. RMS values measured at the *FA_prox* location, computed on each trial, for each player, racket, and ball spin. For each racket (R1, R2, and R3 from left to right), values are ordered according to serve type: *kick* (green, left) and *flat* (copper, right). The values of each player are represented by a single marker. For each player, a cross indicates the mean, and a vertical bar spans the 95% confidence interval around the mean. The black cross and vertical lines indicate the mean and 95% confidence interval around the mean, computed across all players.

4.2. Acoustic and Vibratory Energy

Figures 5 and 6 show the RMS values merged across players, grouped by racket and ball spin, and presented for each accelerometer location on the racket (respectively, on the body).

According to these figures, *flat* serves seemed to produce higher RMS values than *kick* ones. This is confirmed by the RM-ANOVA (see Table 1) showing that for all but the *HIP* and *HOP* accelerometers, the RMS values of *flat* serves were significantly higher than RMS values of *kick* serves (on average 141.53 ± 23.07 g vs. 99.09 ± 21.08 , 136.26 ± 28.67 vs. 78.08 ± 22.08 , 18.66 ± 3.84 vs. 16.36 ± 3.34 , 13.67 ± 2.67 vs. 9.42 ± 2.02 , 13.22 ± 4.41 vs. 10.79 ± 4.18 , 5.38 ± 2.19 vs. 3.74 ± 0.89 , 4.50 ± 2.13 vs. 3.33 ± 0.82 for accelerometer locations *SIP*, *SOP*, *FA_dist*, *FA_prox*, *UA_dist*, *UA_prox*, and *Acromion*, respectively). No significant differences in RMS values were found to depend on the factor *racket* or on the interaction between *racket* and *stroke type*.

According to the Kruskal–Wallis test, RMS values were found to significantly differ between the five accelerometers on the upper limb ($s = 769.11$, $p = 3.77 \times 10^{-165}$): 17.51 ± 3.68 g, 11.55 ± 2.79 , 12.02 ± 4.38 , 4.56 ± 1.79 , and 3.92 ± 1.67 for accelerometer locations *FA_dist*, *FA_prox*, *UA_dist*, *UA_prox*, and *Acromion*, respectively.

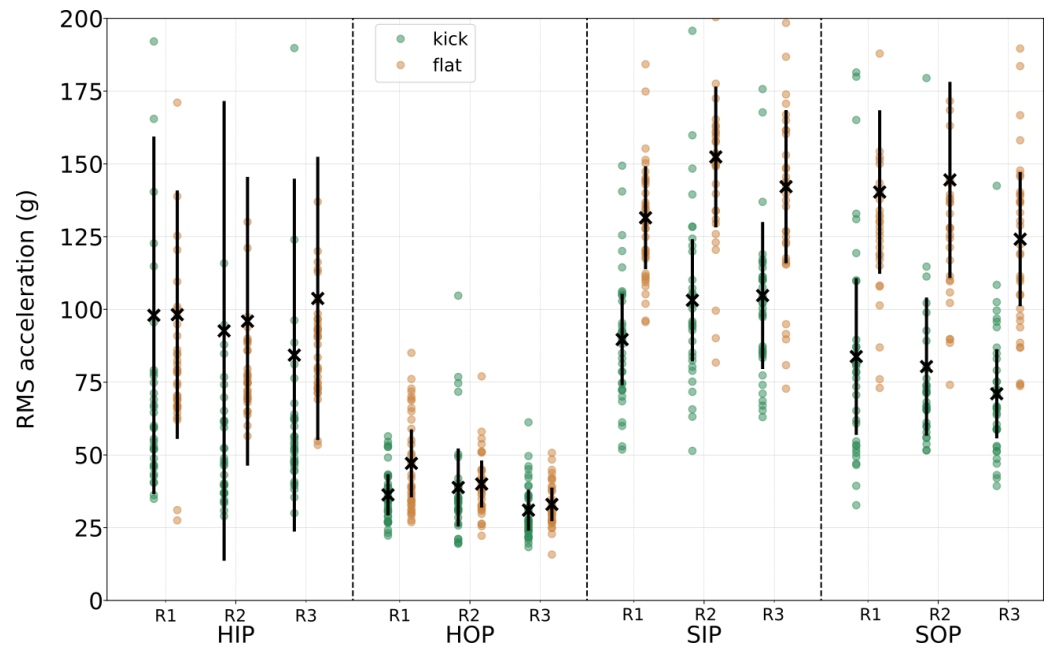


Figure 5. RMS acceleration values, for all trials, players, rackets, ball spin, presented by sensor location on the racket (*HIP, HOP, SIP, SOP*), racket (*R1, R2, R3*), and ball spin (green for *kick*, copper for *flat*). Black crosses and vertical lines indicate, for each distribution, the mean and 95% confidence interval around the mean, respectively.

The Kruskal–Wallis test also found significantly different RMS values between the four accelerometers on the racket ($s = 366.53, p = 3.92 \times 10^{-79}$): 95.36 ± 57.80 g, 37.79 ± 9.46 , 120.61 ± 26.55 , and 107.44 ± 32.60 , for accelerometer locations *HIP, HOP, SIP*, and *SOP*, respectively. Post-hoc Mann–Whitney tests showed that differences were significant within each couple of accelerometers, except between accelerometers at locations *FA_prox* and *UA_dist*, two accelerometers very close to each other.

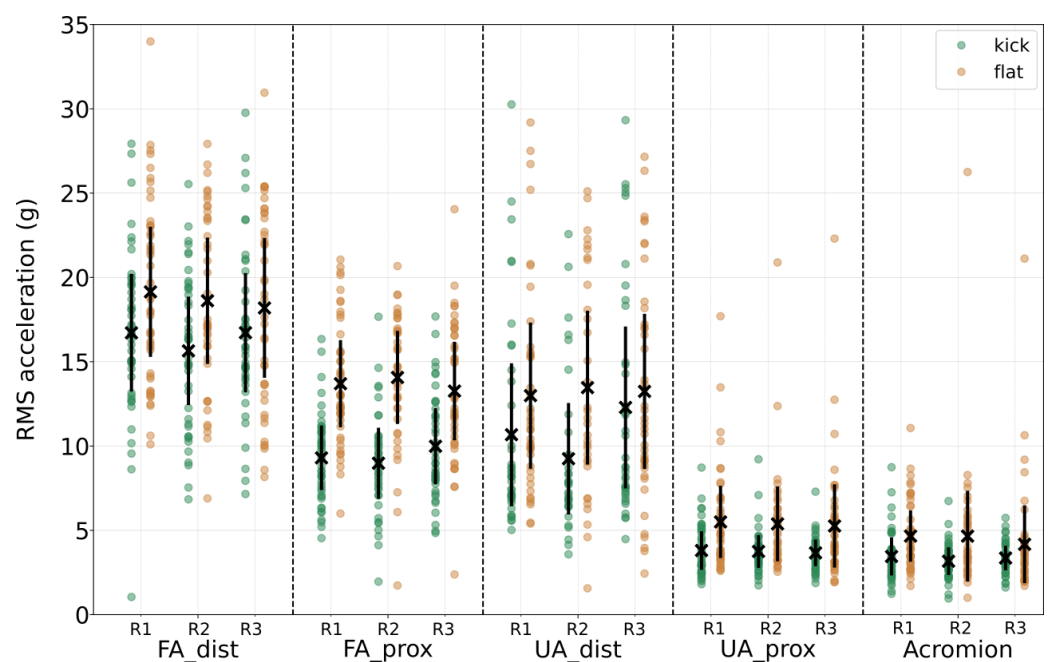


Figure 6. RMS acceleration values, for all trials, players, rackets, ball spin, presented by sensor location on the body (*FA_dist, FA_prox, UA_dist, UA_prox, Acromion*), racket (*R1, R2, R3*), and ball spin (green for *kick*, copper for *flat*). Black crosses and vertical lines indicate, for each distribution, the mean and 95% confidence interval around the mean, respectively.

Table 1. Results of RM-ANOVA tests for vibration descriptors (RMS, SC) computed on data from each accelerometer. First column lists the vibratory descriptors, second column the factors of the RM-ANOVA (R and S stand for factors *racket* and *ball spin*, respectively), third column shows the statistics of the RM-ANOVA, and each following column gives the result for each accelerometer (FA_d, FA_p, UA_d, uA_p, and A stand for *FA_dist*, *FA_prox*, *UA_dist*, *UA_prox*, and *Acromion*, respectively). Underlined are the significant *p*-values.

			HIP	HOP	SIP	SOP	FA_d	FA_p	UA_d	UA_p	A
RMS	R	F(16,2) <i>p</i>	0.52 0.61	3.09 0.05	3.47 0.06	0.56 0.58	0.34 0.71	0.46 0.64	0.56 0.59	1.47 0.26	1.91 0.18
	S	F(8,1) <i>p</i>	0.10 0.76	1.77 0.23	18.32 5×10^{-3}	34.22 1.1×10^{-3}	5.65 <u>0.45</u>	71.93 2.9×10^{-5}	9.58 <u>0.03</u>	7.11 <u>0.03</u>	7.83 <u>0.02</u>
SC	R	F(16,2) <i>p</i>	2.48 0.12	0.55 0.59	5.61 <u>0.02</u>	2.01 0.17	0.23 0.80	2.04 0.16	0.56 0.59	2.86 0.09	2.75 0.09
	S	F(8,1) <i>p</i>	10.69 <u>0.01</u>	9.51 <u>0.02</u>	12.13 <u>0.01</u>	3.01 0.13	1.09 0.33	4.00 0.08	0.97 0.37	1.76 0.22	2.81 0.13

Figure 7 shows the sound level values merged across players, grouped by racket and ball spin. It can be observed that *flat* serves clearly produced higher sound levels (i.e., louder sounds) than *kick* ones. The RM-ANOVA found significant differences between the *flat* and *kick* serves ($F(8,1) = 69.14, p = 3.3 \times 10^{-5}$): 76.82 ± 2.10 dB vs. 71.36 ± 2.57 and 78.84 ± 1.39 dB vs. 73.10 ± 1.79 for *flat* and *kick*, respectively. Difference between rackets were also found ($F(16,2) = 5.03, p = 0.02$): $76.56 \pm 2.43, 75.47 \pm 2.69$, and 75.83 ± 2.48 for R1, R2, and R3, respectively. A Tukey HSD post-hoc test, however, showed no differences between rackets.

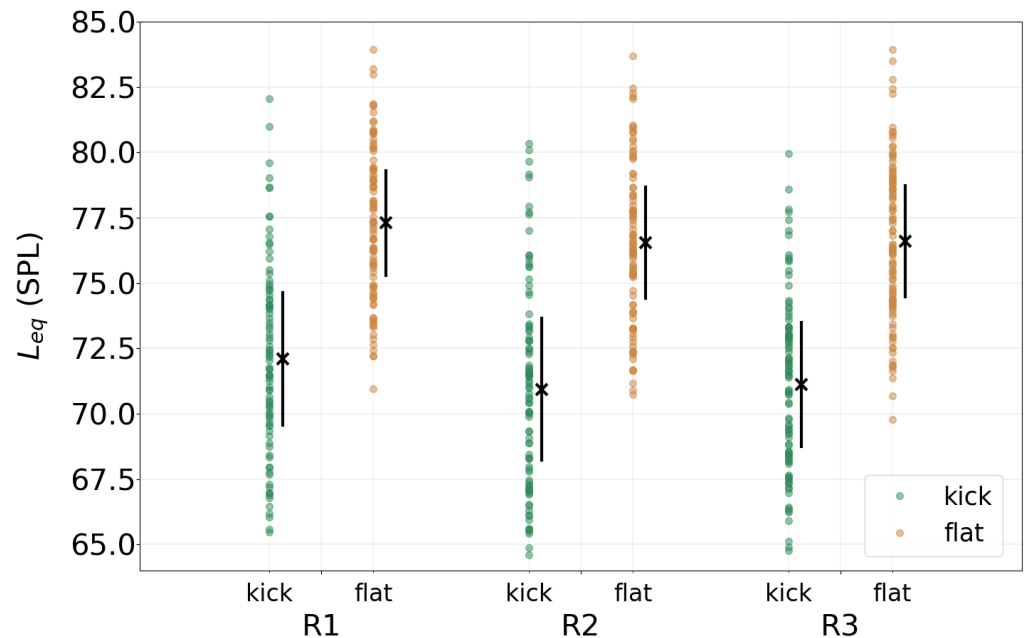


Figure 7. Sound pressure level (L) values, for all trials, players, rackets, ball spin conditions. For each racket (R1, R2, and R3 from left to right), values are ordered according to ball spin: *kick* (green, left) and *flat* (copper, right). The black cross and vertical lines indicate the mean and 95% confidence interval around the mean, computed across all measurements.

4.3. Spectral Features

Figures 8 and 9 show the spectra of the sound recordings, averaged over players and trials, grouped by racket and ball spin, respectively. In Figure 8, the 95% confidence intervals

around the means of *flat* and *kick* spectra do not overlap over the [200–10,000] Hz frequency range (for ease-of-read reasons, spectra are displayed up to 5000 Hz only), showing that the ball spin had an influence on the spectral content. Overall, *flat* serves showed higher amplitudes than *kick* serves over the whole frequency range, testifying to a higher overall sound level, as shown in Section 4.2. Spectra from different ball spin conditions also exhibited different shapes: frequencies around 500 and 900 Hz were reinforced in the spectra for the *flat* serves, whereas the *kick* serves showed a slight amplification around 1000 Hz. On the contrary, Figure 9 shows no influence of the racket on the spectra (slight differences that can be noted, like e.g., R1 showing peaks around 2500 and 4500 Hz, are in fact due to the ball spin).

Similarly, Figures 10 and 11 show the spectra of the vibratory signals measured at the *FA_prox* location (other locations, not shown here, show similar tendencies), averaged over players and trials, and grouped by racket and ball spin, respectively. Figure 10 shows that the ball spin had an influence on the spectral content, and confirms the results of Section 4.2 showing that *flat* serves produced higher vibration levels than *kick* ones, and this held true over the whole frequency range observed here. As was observed for the acoustic spectra, the racket model did not seem to have an influence on the vibratory spectra, as seen in Figure 11, where confidence intervals strongly overlap.

Figure 12 shows the SC values computed on the acoustic signals, merged across player, and grouped according to *racket* and *ball spin*. *Kick* serves produced sounds with higher spectral centroids than *flat* ones. The RM-ANOVA found significant differences between the *kick* and *flat* serves ($F(8,1) = 43.22$, $p = 2 \times 10^{-4}$): $3,213.93 \pm 173.22$ Hz vs. 3790.72 ± 325.76 respectively. Differences between rackets were also found ($F(16,2) = 4.74$, $p = 0.02$): 3522.48 ± 241.67 Hz, and 3590.51 ± 392.96 , 3410.26 ± 322.56 for R1, R2, and R3, respectively. A Tukey HSD post-hoc test showed that racket R2 produced sounds with significantly higher spectral centroids than R3 ($p = 0.01$).

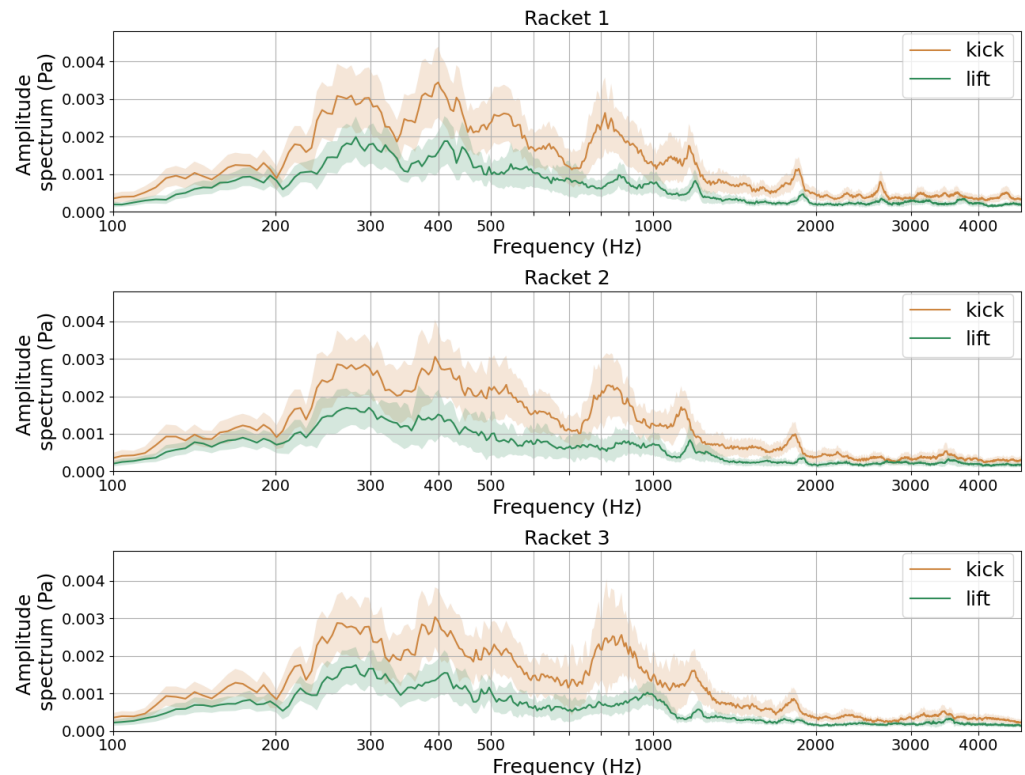


Figure 8. Acoustic spectra, averaged across 8 players. Thick lines show the mean and shaded areas show the 95% confidence interval around the mean. Copper (resp. green) color indicates a *flat* (resp. *kick*) serve. Top, intermediate, and bottom panels, respectively, show spectra for rackets R1, R2, and R3.

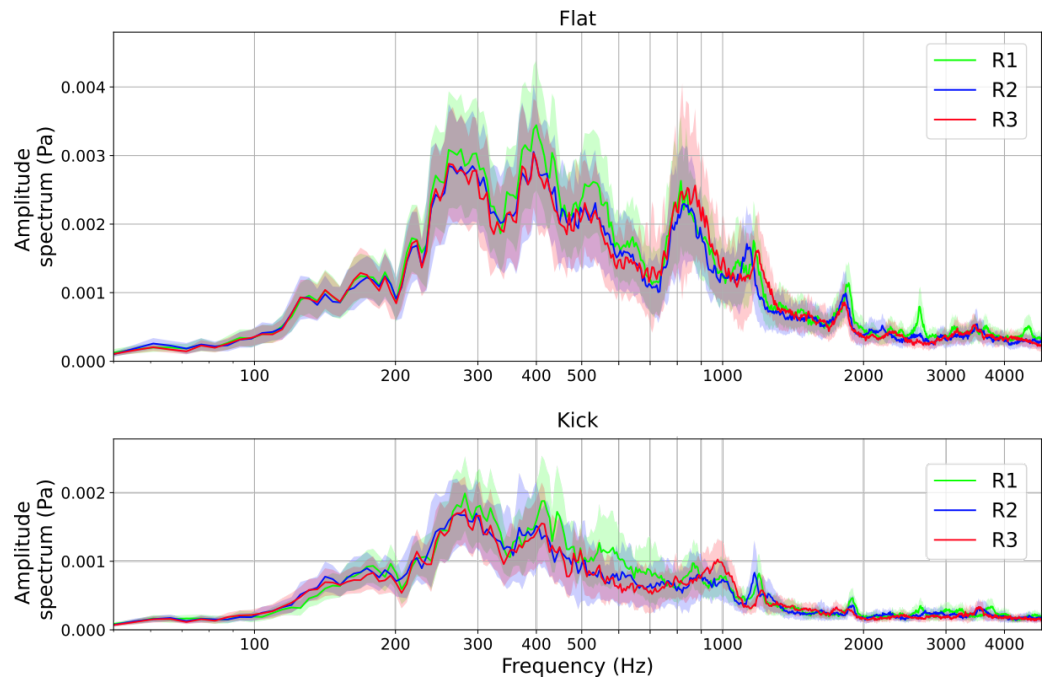


Figure 9. Acoustic spectra, averaged across 8 players. Thick lines show the mean and shaded areas show the 95% confidence interval around the mean. Red, blue, and green colors correspond to spectra of rackets R1, R2, and R3, respectively. Top (resp. bottom) panel shows spectra for *flat* (resp. *kick*) serves.

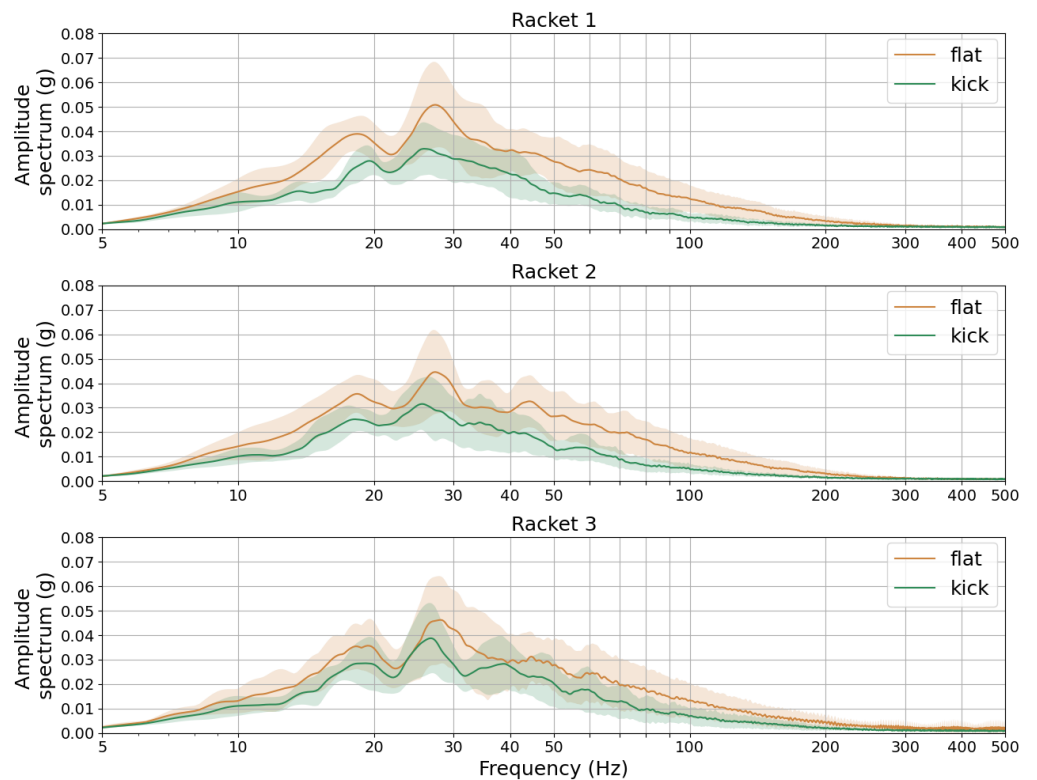


Figure 10. Vibratory spectra for signals measured at the *FA_prox* location, averaged across 8 players. Thick lines show the mean and shaded areas show the 95% confidence interval around the mean. Copper (resp. green) color indicates a *flat* (resp. *kick*) serve. Top, intermediate, and bottom panels respectively show spectra for rackets R1, R2, and R3.

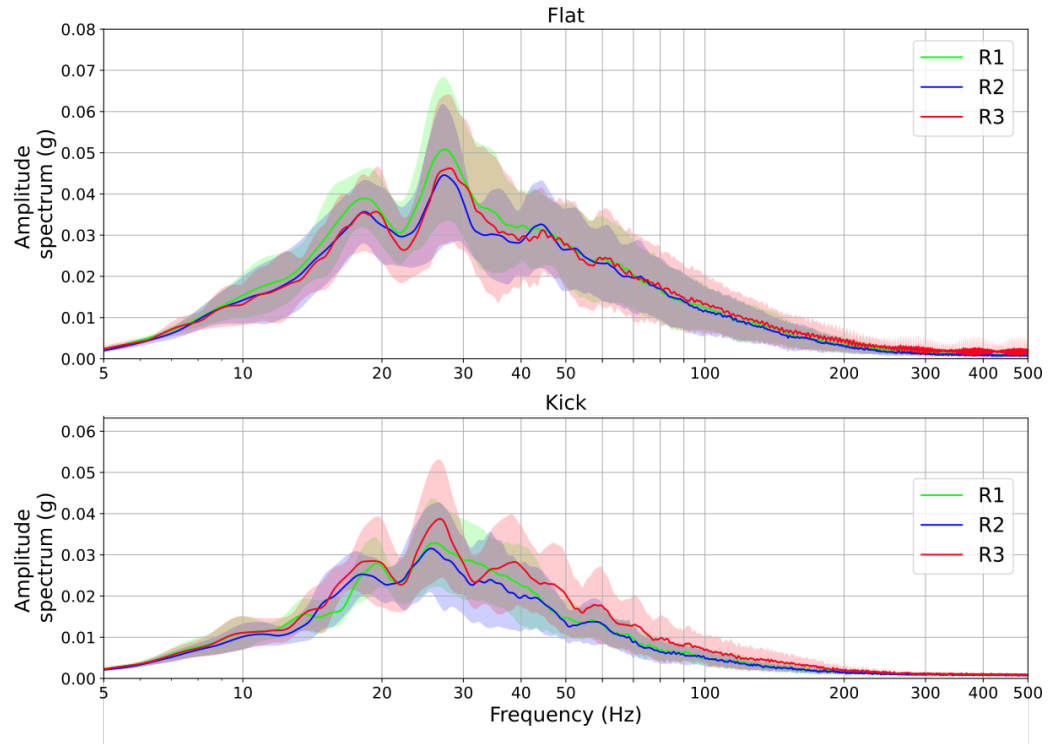


Figure 11. Vibratory spectra for signals measured at the *FA_prox* location, averaged across 8 players. Thick lines show the mean and shaded areas show the 95% confidence interval around the mean. Red, blue, and green colors correspond to spectra of rackets R1, R2, and R3, respectively. Top (resp. bottom) panel shows spectra for *flat* (resp. *kick*) serves.

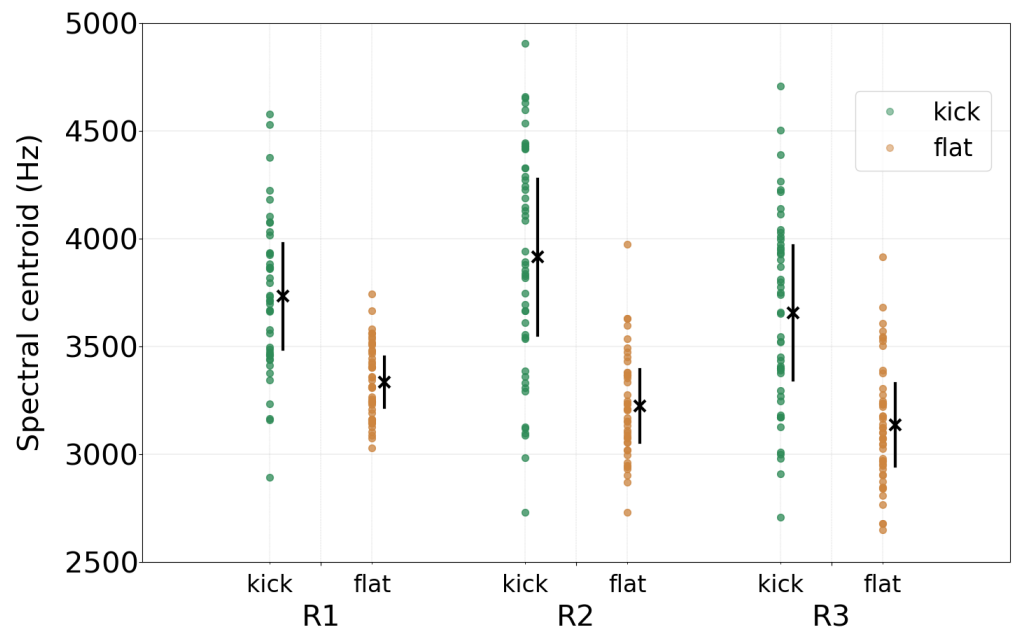


Figure 12. Spectral centroid (SC) values, for all trials, players, rackets, ball spin conditions. For each racket (R1, R2, and R3 from left to right), values are ordered according to serve type: *kick* (green, left) and *flat* (copper, right). The black cross and vertical lines indicate the mean and 95% confidence interval around the mean, computed across all measurements.

Figures 13 and 14 present the SC values for accelerometers located, respectively, on the racket and on the body. The RM-ANOVA showed that *ball spin* had a significant influence on SC values for accelerometers *HIP*, *HOP*, and *SIP*, for which the *flat* serves produced higher SC values than the *kick* serves: 196.09 ± 33.32 Hz vs. 176.49 ± 32.35 , 215.60 ± 36.44 vs. 187.54 ± 44.06 , and 204.99 ± 28.04 vs. 180.37 ± 38.45 , respectively.

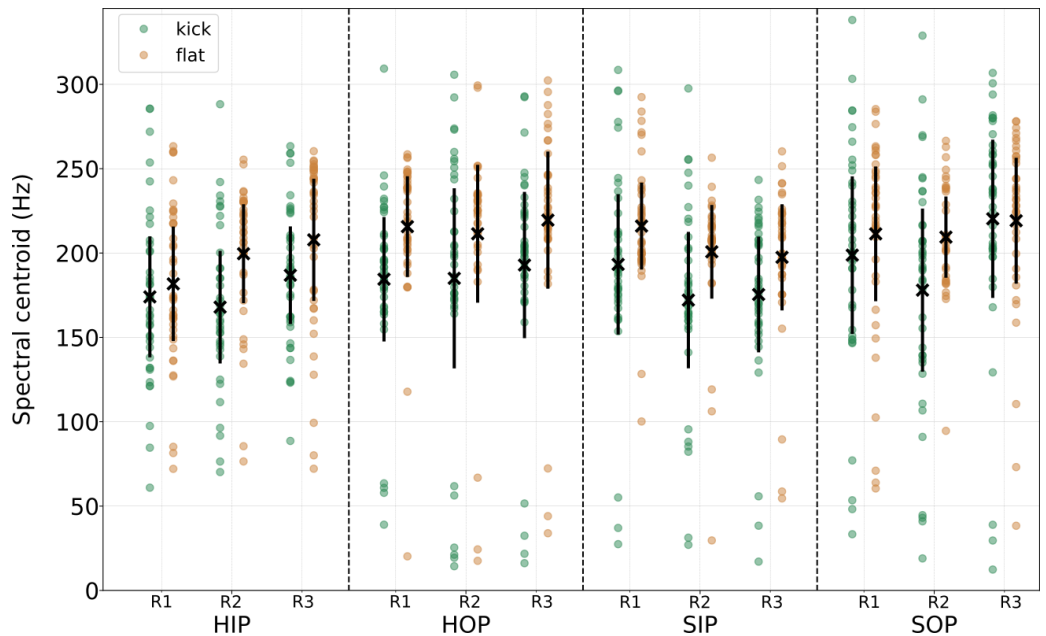


Figure 13. SC values, for all players, presented by sensor location on the racket (*HIP*, *HOP*, *SIP*, *SOP*), racket (*R1*, *R2*, *R3*), and ball spin (green for *kick*, copper for *flat*). Black crosses and vertical lines indicate, for each distribution, the mean and 95% confidence interval around the mean, respectively.

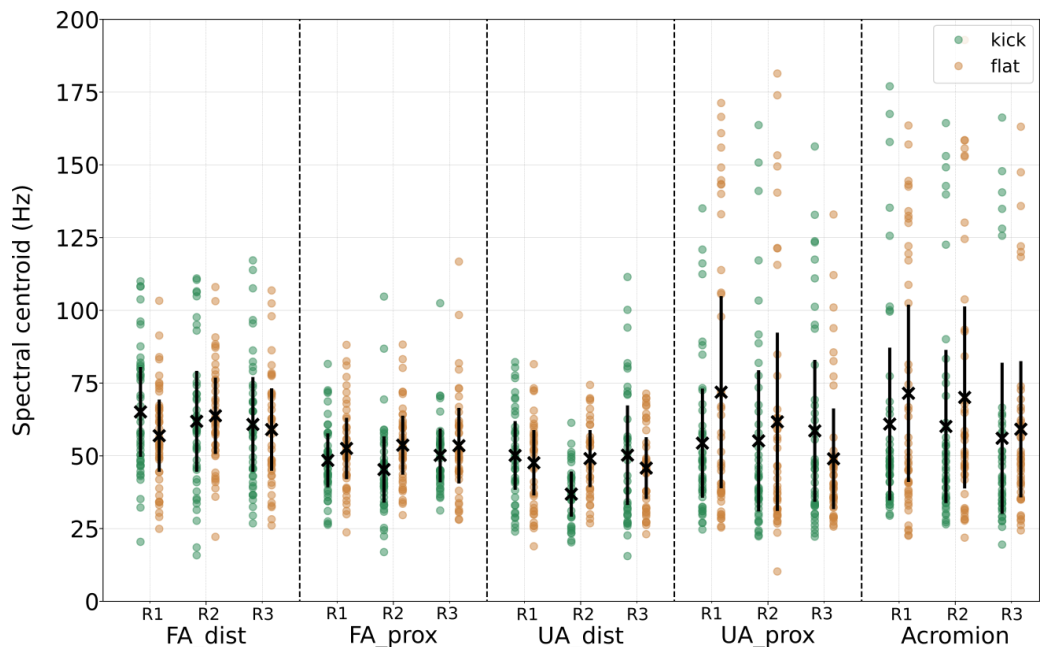


Figure 14. SC values, for all players, presented by sensor location on the body (*FA_dist*, *FA_prox*, *UA_dist*, *UA_prox*, *Acromion*), racket (*R1*, *R2*, *R3*), and ball spin (green for *kick*, copper for *flat*). Black crosses and vertical lines indicate, for each distribution, the mean and 95% confidence interval around the mean, respectively.

Racket type was shown to have a significant influence on SC values for the accelerometer *SIP*. A Tukey HSD post-hoc test showed that *R1* produced vibrations with higher SC values than *R2*: 204.77 ± 34.51 Hz vs. 186.23 ± 35.27 . All other distributions showed no significant differences in terms of SC.

According to the Kruskal–Wallis test on SC values merged across players, trials, rackets and ball spin conditions, SC values were found to significantly differ between the five accelerometers on the upper limb ($s = 72.89$, $p = 5.56 \times 10^{-15}$): 61.24 ± 14.47 Hz, 50.60 ± 10.35 , 46.79 ± 11.69 , 58.52 ± 25.38 , and 63.04 ± 27.19 , respectively, for the *FA_dist*, *FA_prox*, *UA_dist*, *UA_prox*, and *Acromion* locations. SC were also found to significantly differ between the four accelerometers on the racket ($s = 38.94$, $p = 1.79 \times 10^{-8}$): 186.20 ± 33.53 Hz, 201.45 ± 41.61 , 192.57 ± 34.76 , and 206.13 ± 42.05 , respectively for the *HIP*, *HOP*, *SIP*, and *SOP* locations. Post-hoc Mann–Whitney tests showed that differences were significant within each couple of accelerometer locations, except between *FA_prox* and *UA_prox*, *FA_prox* and *Acromion*, *UA_dist* and *UA_prox*, *UA_prox* and *Acromion*, *HIP* and *SIP*, and *HOP* and *SOP*. Interestingly, in-plane (resp. out-of-plane) vibrations on the racket had similar SC values.

4.4. Link between Acoustics and Vibration

Section 4.2 showed that *flat* serves produced significantly louder sounds and higher vibration levels than *kick* ones. Figure 15a shows the sound level values versus RMS vibratory values measured at the *FA_prox* location, computed for each player, racket and ball spin, averaged over trials. It confirms that *flat* serves produced higher levels in both the acoustic and vibratory domains, and that the racket had no influence on these levels. The Pearson correlation coefficient between acoustic and vibratory level amounts to $r = 0.67$ ($p = 2.29 \times 10^{-7}$) and $r = 0.63$ ($p = 6.55 \times 10^{-6}$), which confirms the relationship between levels in both domains. Data from other accelerometer locations all showed positive correlation coefficients between sound level and RMS vibratory values, although only one other case was statistically significant (*HIP*: $r = 0.58$, $p = 6.22 \times 10^{-5}$ $r = 0.53$, $p = 8.92 \times 10^{-4}$).

Figure 15b similarly shows the acoustic SC values against vibratory SC values measured at the *FA_prox* location. It can be observed that higher acoustic SC values tended to be associated with lower vibratory SC values, which is consistent with the results of Section 4.3, showing that *kick* serves produced higher acoustic SC values and lower vibratory SC values. The Pearson correlation coefficient between acoustic and vibratory SC values amounted to $r = -0.28$ ($p = 0.05$) and $r = -0.23$ ($p = 0.15$), a negative correlation coefficient in line with the mentioned trend, and hardly but not statistically significant. Data from other accelerometer locations all showed negative correlation coefficients between acoustic and vibratory SC values, although, again, only one other case was statistically significant (*HOP*: $r = -0.33$, $p = 0.04$ *FA_dist*: $r = -0.30$, $p = 0.05$).

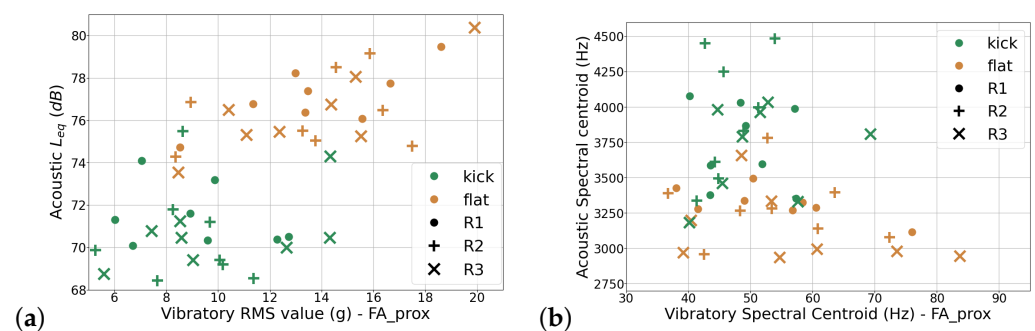


Figure 15. Sound level vs. RMS vibratory values measured at the *FA_prox* location (a), acoustic SC vs. vibratory SC measured at the *FA_prox* location (b). Markers represent the mean across trials for each player/racket/ball spin combination. Color indicates ball spin: *kick* in green, *flat* in copper. Markers indicate rackets: filled circle for *R1*, upright cross for *R2*, x for *R3*.

5. Discussion

The first objective of the study was to evaluate shock-induced vibration propagation from the racket to the player's shoulder with respect to various serve conditions (*racket* and *ball spin*). As expected and consistently with the literature, results confirmed that the further the accelerometer on the upper limb from the impact point, the lower the level of transmitted vibration (see e.g., [1,9,10]). A contribution of the present study was to assess the vibration propagation up to the player's shoulder and not only to the player's elbow. It reveals that the shock-induced vibration persists and can be measured at the shoulder level, influenced by the serve conditions. Despite the estimated RMS levels being low (less than 5 g), this raises the possibility of investigating injury risk and comfort levels at the upper arm. Further, while the racket had no clear effect on the vibration propagating through the upper limb, the ball spin clearly affected the results, with a flat serve inducing higher RMS level than a kick serve. The ball spin effect was also highlighted by [4]: a flat stroke produced a higher acceleration peak at the racket's head compared to a topspin stroke, while the opposite was observed at the joint level (articulations). Interestingly, almost no difference was observed on the racket's handle with respect to the investigated conditions. On the contrary, the racket's head vibration reflected the serve conditions, especially the ball spin. Again, a flat serve induced a higher RMS level than a kick serve. However, contrary to our expectations, the energy repartition between the in-plane and out-of-plane vibrations was not correlated to the ball spin. Further research should more precisely control the ball rotation and speed to gain a deeper understanding of this issue. Further, in-plane (IP) vibrations had higher levels than out-of-plane (OP) vibrations, which was quite unexpected given that the excitation was deemed to be in the out-of-plane direction. However, as discussed in [13], in-plane excitation may well be non negligible with top-spin serves. It was also observed that in-plane and out-of-plane vibrations on the racket had similar SC values. This indicates a similar distribution of vibrating energy in the spectral domain for both directions of vibration, which may be due to the rackets showing similar modal frequencies and amplitudes in the in-plane and in the out-of-plane directions. Due to constraints of time and availability of rackets, no modal analysis could be conducted on the three rackets, so this hypothesis can not be verified.

The second objective of the study was to investigate if and how contactless, non-invasive, acoustic measurements may be used instead of invasive vibratory measurements. This would require the acoustic and vibratory measurements to consistently show similar trends. Here, acoustic and vibratory levels were found to be correlated, which is not surprising as the radiated sound waves result from the vibration of the radiating solid (here, a strung racket). A racket vibrating more strongly radiates louder and transmits more vibratory energy to the upper limb. In terms of spectral content, acoustic and vibratory SC values tended to behave in opposite ways: vibrations with higher SC values produced sounds with lower SC values. This was rather unexpected (as the vibratory spectrum and the resulting sound spectrum are supposed to be somehow similar), and several explaining hypotheses might be put forward that cannot be tested in the present study: the radiation pattern due to the vibroacoustic coupling of a complex object (racket made of composite material, with vibration patterns due to the modes of the frame as well as the strings) might result in strong spectral modifications from the vibratory spectrum to the acoustic spectrum, and the radiation pattern might strongly depend on the relative locations (distance, angle) of the microphone and the impact point. Although we assumed the routine serve gesture of each expert player to be repeatable enough so as to minimize the variation in the impact/microphone relative location, further studies may consider recording the sound with in-ear microphones in order to get rid of this source of variability. Additionally, here, the frequency ranges investigated in the vibratory and acoustic measurement were very different. Further studies should investigate further the link between acoustic and vibration, possibly through more controlled experiments and modeling, e.g., vibration sensing at more points and in all directions, acoustic measurements in anechoic chambers, control of the directivity of microphones, measurements with other microphone locations

(either fixed at longer distance from impact point to ensure far-field propagation conditions, or using intra-aural microphones worn by the player to insure constant distance from impact point), investigation of the exact same frequency range for acoustics and vibration, analytical or numerical modeling of vibro-acoustic coupling, and the measurement of ball speed after impact and/or impact force between the racket and the ball.

If in the future some acoustic features are confirmed to be acceptable proxies for vibratory features (which may in the end happen, as, e.g., ref. [14] established a solid relationship between the vibratory and acoustic spectra of the racket/ball impact in table tennis), methods involving listening to the impact sounds (i.e., perception tests and psychological and psychoacoustical measurements) instead of measuring them with physical devices can also be considered. Higher sound levels of *flat* serves may well be perceived as louder by human listeners. Additionally, higher SC values (i.e., sounds with energy concentrated more in the higher frequencies) of *kick* serve sounds might be perceived as “brighter”, and the lower-SC sounds of *flat* serves might be perceived as “duller” or “more muffled”. Such differences were actually heard by authors and players during the experiments.

Even if some differences could be highlighted in the vibratory measurements, these differences were in general quite small: RMS and SC values for the accelerometers on the racket were very similar from one accelerometer to another; differences between rackets could only rarely be sensed. On the contrary, during informal discussion, the players involved in this study claimed to be capable of clearly perceiving vibration differences between rackets and ball spin conditions. This indicates that, as of the day of writing, our physical measurements have a much lower discrimination power than the players' perception does. It could be that the descriptors that were used in this study were too simplistic, and other descriptors should be tested in future studies, e.g., spectral descriptors not reducing the spectra to a single value (as the SC does), or temporal descriptors such as the decay time. It may also be that the players adapt their gestures, grip position, and grip force to the different conditions [10], so as to adapt the amount of transmitted vibration in order to improve their comfort, reducing the differences that physical devices may sense. Further studies should also investigate how players feel and perceive the radiated sound and transmitted vibration, in order to confirm whether they actually can perceive differences between conditions, and how they achieve this (relying on which aspects of sound and vibration). Taking into account the players' auditory perception seems like a very promising approach. Sound perception has indeed been shown to be quite important in the sport domain, whether it be for rehabilitation or training [15,16], for using the impact sound as an indicator of the quality of the equipment [17–19], or for using auditory cues to predict the opponent's actions [20].

6. Conclusions

The first objective of the study was to assess the vibration propagation from the racket to the player's shoulder during a tennis serve. For this purpose, eight expert tennis players were asked to perform serves with three rackets (selected for their contrasting vibratory behavior) and two ball spin conditions (*flat* and *kick*) to mimic a wide range of admissible excitation. Sound and vibration signals were analyzed in terms of simple descriptors, namely, the level (sound pressure level L , RMS level) and the spectral centroid (SC). Results underlined a significant influence of the ball spin on both the level (*flat* serves producing louder sounds and higher vibration levels than *kick* ones) and the spectrum (*flat* serves producing lower acoustic SC values and higher vibratory SC values than *kick* ones). The *racket* factor was shown to have but a marginal influence. Beyond the spectral centroid, the shape of the spectra also depended on the ball spin and not on the racket. The second objective of the study was to link acoustic and vibratory measurements. Similarities between both measurements were found (sound and vibration levels were correlated), but also differences (SC sound and vibration values tended to be negatively correlated) that remain to be explained. Further studies should therefore investigate more in detail

the link between sound and vibration, possibly using more controlled experiments or perceptual tests.

Author Contributions: A.P., M.P. and D.C. conceived the study. A.P., M.P. and D.C. planned the study. A.P., M.P., N.B. and D.C. participated in the preliminary and the main experiments. A.P. and D.C. analyzed and interpreted the data and wrote the article. All authors have read and agreed to the published version of the manuscript.

Funding: This research received no external funding.

Institutional Review Board Statement: The experiment in this study was approved by the national ethic committee, under number IRB00012476-2022-24-05-184.

Informed Consent Statement: Informed consent was obtained from all players involved in the study.

Data Availability Statement: Data of this study can be made available upon reasonable request to the corresponding author.

Acknowledgments: The authors thank the players who volunteered for the measurements, as well as Thomas Daney for fruitful discussions and Lucie Lesecq for help during preliminary experiments.

Conflicts of Interest: The authors declare no conflicts of interest.

Abbreviations

SC: spectral centroid; L: sound level; HIP: Handle In-Plane; HOP: Handle Out-of-Plane; SIP: Side of frame In-Plane; SOP: Side of frame Out-of-Plane

References

- Hennig, E.; Rosenbaum, D.; Milani, T. Transfer of tennis racket vibrations onto the human forearm. *Med. Sci. Sport. Exerc.* **1992**, *24*, 1134–1140. [[CrossRef](#)]
- Yeh, I.-L.; Elangovan, N.; Feczer, R.; Khosravani, S.; Mahnan, A.; Konczak, J. Vibration-Damping technology in tennis racquets: Effects on vibration transfer to the arm, muscle fatigue and tennis performance. *Sport. Med. Health Sci.* **2019**, *1*, 49–58. [[CrossRef](#)] [[PubMed](#)]
- Taraborrelli, L.; Grant, R.; Sullivan, M.; Choppin, S.; Spurr, J.; Haake, S.; Allen, T. Materials Have Driven the Historical Development of the Tennis Racket. *Appl. Sci.* **2019**, *9*, 4352. [[CrossRef](#)]
- Rigozzi, C.J.; Vio, G.A.; Poronnik, P. Comparison of Grip Strength, Forearm Muscle Activity, and Shock Transmission between the Forehand Stroke Technique of Experienced and Recreational Tennis Players Using a Novel Wearable Device. *Sensors* **2023**, *23*, 5146. [[CrossRef](#)] [[PubMed](#)]
- Goisard de Monsabert, B.; Herbaut, A.; Cartier, T.; Vigouroux, L. Electromyography-informed musculoskeletal modeling provides new insight into hand tendon forces during tennis forehand. *Scand. J. Med. Sci. Sport.* **2023**, *33*, 1958–1975. [[CrossRef](#)]
- Chadefaux, D.; Rao, G.; Le Carrou, J.-L.; Berton, E.; Vigouroux, L. The effects of player grip on the dynamic behaviour of a tennis racket. *J. Sport. Sci.* **2016**, *35*, 1155–1164.
- Pedro, B.; Cabral, S.; Veloso, A.P. Concurrent validity of an inertial measurement system in tennis forehand drive. *J. Biomech.* **2021**, *121*, 110410. [[CrossRef](#)]
- Martin, C. Biomechanics of the Tennis Serve. *Tennis Med.* **2018**, *316*. _1 [[CrossRef](#)]
- Wei, S.-H.; Chiang, J.-Y.; Shiang, T.-Y.; Chang, H.-Y. Comparison of Shock Transmission and Forearm Electromyography Between Experienced and Recreational Tennis Players During Backhand Strokes. *Clin. J. Sport Med.* **2006**, *16*, 129–135. [[CrossRef](#)] [[PubMed](#)]
- Chadefaux, D.; Rao, G.; Androuet, P.; Berton, E.; Vigouroux, L. Active tuning of stroke-induced vibrations by tennis players. *J. Sport. Sci.* **2016**, *35*, 1643–1651. [[CrossRef](#)] [[PubMed](#)]
- Rogowski, I.; Creveaux, T.; Triquigneaux, S.; Macé, P.; Gauthier, F.; Sevez, V. Tennis Racket Vibrations and Shock Transmission to the Wrist during Forehand Drive. *PLoS ONE* **2015**, *10*, e0132925. [[CrossRef](#)] [[PubMed](#)]
- Chung, K.C.; Lark, M.E. Upper Extremity Injuries in Tennis Players: Diagnosis, Treatment, and Management. *Hand Clin.* **2017**, *33*, 175–186. [[CrossRef](#)] [[PubMed](#)]
- Banwell, G.H.; Roberts, J.R.; Halkon, B.J.; Rothberg, S.J.; Mohr, S. Understanding the Dynamic Behaviour of a Tennis Racket under Play Conditions. *Exp. Mech.* **2014**, *54*, 527–537. [[CrossRef](#)]
- Manin, L.; Poggi, M.; Bertrand, C.; Havard, N. Vibro-acoustic of table tennis rackets. Influence of the plywood design parameters. Experimental and sensory analyses. *Procedia Eng.* **2014**, *72*, 374–379. [[CrossRef](#)]
- Sors, F.; Murgia, M.; Santoro, I.; Agostini, T. Audio-Based Interventions in Sport. *Open Psychol. J.* **2015**, *8*, 212–219. [[CrossRef](#)]
- Schaffert, N.; Braun Janzen, T.; Mattes, K.; Thaut, M.H. A Review on the Relationship Between Sound and Movement in Sports and Rehabilitation. *Front. Psychol.* **2019**, *10*, 244. [[CrossRef](#)]

17. Roberts, J.R.; Jones, R.; Rothberg, S.J.; Mansfield, N.J.; Meyer, C. Influence of sound and vibration from sports impacts on players' perceptions of equipment quality. *J. Mater. Des. Appl.* **2006**, *220*, 215–227. [[CrossRef](#)]
18. Roberts, J.R.; Jones, R.; Mansfield, N.J.; Rothberg, S.J. Evaluation of vibrotactile sensations in the feel of a golf shot. *J. Sound Vib.* **2005**, *285*, 303–319. [[CrossRef](#)]
19. Roberts, J.R.; Jones, R.; Mansfield, N.J.; Rothberg, S.J. Evaluation of impact sound of the 'feel' of a golf shot. *J. Sound Vib.* **2005**, *287*, 651–666. [[CrossRef](#)]
20. Cañal-Bruland, R.; Müller, F.; Lach, B.; Spence, C. Auditory contributions to visual anticipation in tennis. *Psychol. Sport Exerc.* **2018**, *36*, 100–103. [[CrossRef](#)]

Disclaimer/Publisher's Note: The statements, opinions and data contained in all publications are solely those of the individual author(s) and contributor(s) and not of MDPI and/or the editor(s). MDPI and/or the editor(s) disclaim responsibility for any injury to people or property resulting from any ideas, methods, instructions or products referred to in the content.